What Are the Reasons for the Kinetic Stability of a Mixture of H_2 and O_2?

Michael Filatov,[†] Werner Reckien,[‡] Sigrid D. Peyerimhoff,*[,‡] and Sason Shaik*[,†]

Department of Organic Chemistry and The Lise Meitner-Minerva Center for Computational Quantum Chemistry, Hebrew University, 91904 Jerusalem, Israel, and Institut für Physikalische und Theoretische Chemie der Universität Bonn, Wegelerstrasse 12, 53115 Bonn, Germany

Received: September 13, 2000

Calculations at the (14,10)CASSCF/6-31G** and the MR-(S)DCI/cc-pVTZ levels are employed to answer the title question by studying three possible modes of reaction between dioxygen and dihydrogen molecules at the ground triplet state and excited singlet state of O_2. These reaction modes, which are analogous to well-established mechanisms for oxidants such as transition metal oxene cations and mono-oxygenase enzymes, are the following: (i) the concerted addition, (ii) the oxene-insertion, and (iii) the hydrogen abstraction followed by hydrogen rebound. The "rebound" mechanism is found to be the most preferable of the three mechanisms. However, the barrier of the H-abstraction step is substantial both for the triplet and the singlet states of O_2, and the process is highly endothermic (>30 kcal/mol) and is unlikely to proceed at ambient conditions. The calculations revealed also that the lowest singlet state of O_2 has very high barriers for reaction and therefore cannot mediate a facile oxidation of H_2 in contrast to transition metal oxenide cation catalysts and mono-oxygenase enzymes. This fundamental difference is explained.

1. Introduction

Spontaneous but slow are the two words used frequently to characterize reactions of the molecular oxygen with hydrogen and other organic molecules.[1] Indeed, from the thermodynamic point of view, the reactions that produce water

$$2H_2 + O_2 \rightarrow 2H_2O \quad (1)$$

or hydrogen peroxide

$$H_2 + O_2 \rightarrow H_2O_2 \quad (2)$$

are exothermic by at least −30 kcal/mol and could be defined thereby as spontaneous. Were thermodynamics the decisive factor of reactivity, these reactions would have been extremely fast. Nevertheless, the reactions are kinetically very slow and mixtures of O_2/H_2 or of O_2 with an organic and living matter are persistent or "kinetically stable" and exist for a sufficiently long time at ambient conditions.[1] In contrast, transition metal catalysts and mono-oxygenase enzymes use O_2 and mediated controlled "slow burning"[2−7] of organic material. Thus, the Damocles sword of O_2 that potentially hovers over life becomes instead the life-sustaining species. The origins of the kinetic stability of the O_2/H_2 mixture is therefore intriguing, and its understanding vis à vis the oxidation processes that are mediated by enzymes and catalysts is an important goal.

The simplest explanation for the kinetic stability of the O_2/H_2 mixture is the spin-forbiddenness of the reactions (e.g., eqs 1 and 2) of molecular oxygen which possesses a triplet ground state, $^3\Sigma_g^-$.[8] This implies that the interaction of molecular oxygen with the substrate results in radical pairs, but this may be quite an endothermic process. Alternatively, spin-interconversion could possibly occur en route to the singlet state products of oxidation. Indeed, dioxygen possesses a low-lying singlet excited state, the $^1\Delta_g$ state, at 0.98 eV above the ground $^3\Sigma_g^-$ state.[8] The reaction on the singlet surface may therefore lead directly to the most stable oxidation products bypassing the formation of radical pairs. On the basis of the Bell−Evans−Polanyi rule,[9] the barriers on the singlet surface are expected to be lower as compared to the triplet barriers. Thus, in principle, had there existed an efficient spin-interconversion mechanism, the singlet state reactivity would have mediated the overall oxidation. However, a spin-interconversion rate depends on the spin−orbit coupling (SOC) as well as on the height of the singlet−triplet crossing point.[10] High energy crossing point and/or small SOC will result in an inefficient reaction under ambient conditions. Is this possibility so inefficient for O_2/H_2 and, if so, why?

A sluggish spin-interconversion mechanism is involved, for example, in the oxidation of H_2 and CH_4 by FeO^+, and the efficiency increases to unity with higher hydrocarbons. FeO^+ possesses the same bonding mechanism as in the ground-state O_2 molecule.[7,10a,d−g] Thus, for FeO^+ and for example, H_2 or CH_4, the reaction proceeds through the spin-junctions between the sextet ground state and the low-lying quartet state.[7,10] The low-spin state cuts across the high-spin surface and provides a low energy pathway. While the overall reaction rate for H_2 and CH_4 oxidation is small because of ineffective SOC, for other alkanes every collision with FeO^+ leads to oxidation.[7] Similarly, enzymes such as cytochrome P450, activate oxygen to a ferryl-oxene species, which has an FeO unit bonded in a manner analogous to O_2, and perform efficient oxidations.[2−6,11] In fact, even H_2 is oxidized by model species of the ferryl oxene.[12] Why then does O_2 appear incapable of oxidizing H_2?

Although the reactions of molecular oxygen are extremely important for chemistry, we did not find in the literature a detailed theoretical study of the initial steps of the reactions in eqs 1 and 2. Is the formation of the radical pairs unavoidable during these reactions or under certain conditions direct oxygen

* To whom correspondence should be addressed.
[†] Hebrew University.
[‡] Universität Bonn.

10.1021/jp0032208 CCC: $19.00
Published on Web 12/05/2000

insertion may occur? Does the singlet state reactivity help to oxidize the substrates, or does it not? In the present paper, we try to address these questions in the quantum−chemical study of the simplest reaction of molecular oxygen, the $H_2 + O_2$ reaction. Deeper understanding of the initial steps of this reaction can be important for atmospheric chemistry, for combustion chemistry, for a large variety of biological oxygenation problems, etc.

Three modes of interaction between one oxygen and one hydrogen molecules are considered by analogy to the oxidation mechanisms by free oxo-metal cations and analogous enzymatic species:[2−7] (i) the concerted addition, (ii) the oxene-insertion, and (iii) the "rebound" mechanisms. Since the oxygen molecule in its ground $^3\Sigma_g^-$ state and the lowest excited singlet $^1\Delta_g$ state has an open electronic shell and since many of the reaction intermediates are typified by strong nondynamic correlation, the method of choice in this paper is the complete active space SCF (CASSCF) calculation. Higher level multireference configuration interaction, MR-(S)DCI, calculations are used for energy evaluation of the critical species with inclusion of dynamic correlation.

2. Details of Calculations

All calculations have been done at the (14,10)CASSCF level and include all valence electrons and all valence orbitals of O_2 and H_2. The CASSCF calculations have been performed with the MOLPRO2000.1[13] and GAMESS-US[14] program packages and employ the 6-31G** basis set.[15] The molecular structures of all critical species were optimized at the CASSCF level. The transition states were sought with the eigenvector following algorithm and were characterized by subsequent vibrational analyses at the CASSCF level.

For the critical species optimized with CASSCF, the single point MR-(S)DCI calculations have been done with the help of the DIESEL-CI program.[16] The MR-(S)DCI calculations employ the cc-pVTZ basis set.[17] The Davidson's correction[18] is added to the MR-(S)DCI total energies. All critical species have been characterized by a vibrational analysis at the (14,10)-CASSCF/6-31G** level. When calculated the energy differences, the CASSCF zero-point vibrational energies were taken into account.

The trajectories for the three reaction mechanisms are defined in Scheme 1. The symmetry along the concerted addition pathway is C_2, and C_s along the oxene-insertion route. No symmetry constraint was imposed on the species from the "rebound" pathway. Two potential surfaces, triplet and singlet, are considered. The ground state of the oxygen molecule, $^3\Sigma_g^-$, becomes ^{3}B in C_2 and ^{3}A" in C_s, and these triplet states were considered for the corresponding trajectories. The lowest singlet excited state, $^1\Delta_g$, of the oxygen molecule has an ^{1}A symmetry in C_2 and ^{1}A′ in C_s. These symmetry constraints were imposed on the singlet C_2 or C_s symmetric species. For the nonsymmetric species, the lowest triplet and singlet states were calculated.

3. Results and Discussion

The results of the CASSCF calculations for the concerted addition, oxene insertion, and rebound mechanisms are summarized in Figures 1 and 2 and Schemes 2 and 3. All the products (**P**) that can emerge from an interaction of the reactants (**R**), one O_2 and one H_2, were calculated. The transition states ($^{2S+1}$**TS$_i$**), reactants ($^{2S+1}$**R$_i$**), and products ($^{2S+1}$**P$_i$**) are marked by their total spin multiplicity ($2S + 1$) and by a respective number (i) given as a subscript. The relative energies in Schemes 2 and 3 are scaled with respect to the triplet state oxygen and

SCHEME 1: Trajectories Used to Study the Oxidation Mechanisms

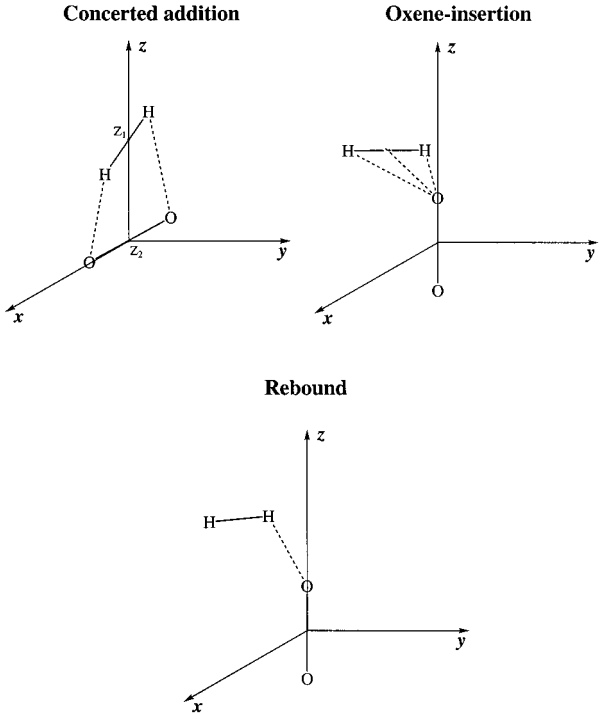

singlet state hydrogen molecules (**^{3}R**). In Schemes 2 and 3, the critical species that belong to the concerted addition mechanism are connected by dashed lines, those from the oxene-insertion mechanism by wavy lines, while those from the rebound mechanism by solid lines.

In general, the transition states are lower in the more extensive MR-(S)DCI treatment, which is expected because both types of correlation energy, static and dynamic, are accounted for to a larger extent than in the CASSCF procedure. Smaller discrepancies between the two methods are observed for the various minima on the potential energy surfaces, with the exception perhaps of **^{1}P$_3$** where the MR-(S)DCI relative energy is 10 kcal/mol lower than the CASSCF one. The calculated MR-(S)DCI energy differences between different species are in nice agreement with the experimental values. Thus, for the dissociation of H_2O_2 (**^{1}P$_3$**) to two OH radicals (**^{1}P$_5$**) MR-(S)-DCI predicts the energy of 42.8 kcal/mol and for the H_2O_2 dissociation to $H + HO_2$ radical pair (**^{1}P$_1$**) it yields 80.5 kcal/mol. Both values compare reasonably with experimentally obtained values of 48.9 and 89.5 kcal/mol,[19] respectively. A recent survey of gas kinetic data[20] lists $\Delta H° = -71.2$ kJ/mol (−17.0 kcal/mol) for $OH + OH \rightarrow H_2O + O$ reaction, which is well-represented by the **^{3}P$_5$** → **^{3}P$_4$** difference of −15.3 kcal/mol from MR-(S)DCI. Furthermore, the $\Delta H° = -233$ kJ/mol (−55.7 kcal/mol)[20] for $H + HO_2 \rightarrow H_2 + O_2$ compares well with the MR-(S)DCI value of −58.0 kcal/mol (see Scheme 2). Thus, as shown by comparison with the available experimental data, the calculated relative energies are quite accurate. Hereafter, in the text itself, the relative energies from the CASSCF calculations will be given without parentheses and the MR-(S)-DCI relative energies are given parenthetically.

1. Concerted Addition Mechanism. A coordinate system for the concerted mechanism is shown in Scheme 1. The *z* axis passes through the median points, Z_1 and Z_2, of the H−H and O−O bonds. The Z_1Z_2 distance between the median points, the O−O and H−H bond lengths, and a twisting angle HZ_1Z_2O

SCHEME 2: Rebound (Solid line), Oxene Insertion (Wavy Line), and Concerted Addition (Dashed Line) on the Triplet Surface[a]

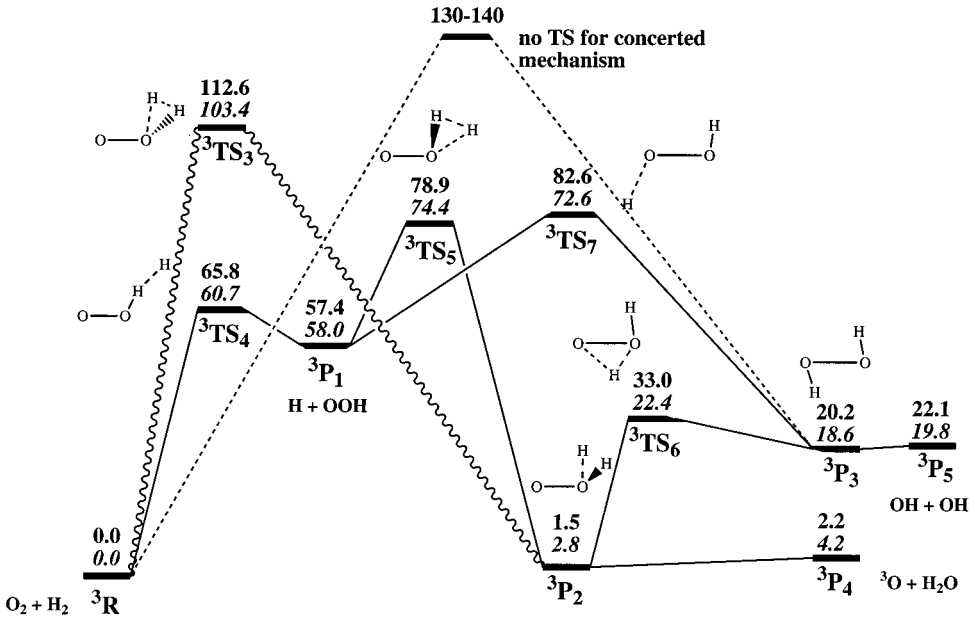

[a] CASSCF values are given in normal font and the MR-(S)DCI values are italicized.

SCHEME 3: Rebound (Solid Line), Oxene Insertion (Wavy Line), and Concerted Addition (Dashed Line) on the Singlet Surface[a]

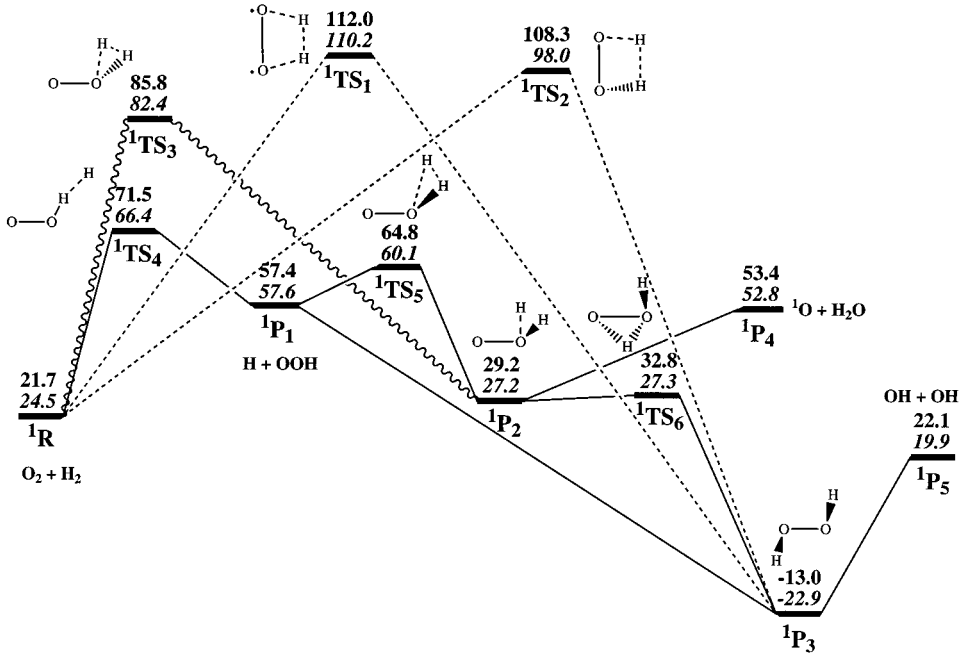

[a] CASSCF values are given in normal font and the MR-(S)DCI values are italicized.

were considered as independent geometry variables, such that the C_2 symmetry is preserved along this pathway.

First, let us consider the triplet potential energy surface, of the concerted mechanism. Under the C_2 symmetry, the states of H_2 and O_2 are the ^{1}A and ^{3}B, respectively. The concerted addition finalizes at hydrogen peroxide molecule ^{3}**P$_3$** in its lowest triplet state, ^{3}B state. In this state, the two OH fragments are weakly bound due to the O···H electrostatic interaction, much like in hydrogen bonds. The O···O distance optimized at the (14,10)CASSCF/6-31G** level is 2.988 Å, the O−H bond length is 0.978 Å, the molecule is planar and the OH fragments are rotated toward one another such that the HOO valence angle is only 50.4° (see Figure 1). The dissociation energy with respect to two OH radicals is only 1.9 kcal/mol at the (14,10)CASSCF/6-31G** level and 1.2 kcal/mol at the MR-(S)DCI/cc-pVTZ level. The reaction is endothermic, 20.2 kcal/mol at the (14,10)-CASSCF/6-31G** level and 18.6 kcal/mol at the MR-(S)DCI/cc-pVTZ level (See Scheme 2).

Despite the fact that the concerted addition starts and ends continuously in the same ^{3}B state, the reaction is symmetry-forbidden. This is illustrated in Scheme 4 where the active orbitals of the reactants ^{3}**R** and product ^{3}**P$_3$** are sketched (the oxygen 2s orbitals are omitted for simplicity). Along the reaction pathway, the number of doubly occupied and empty orbitals of *a* and *b* symmetry changes, such that one of the initially filled *a* orbitals becomes empty and one of the empty *b* orbitals gets

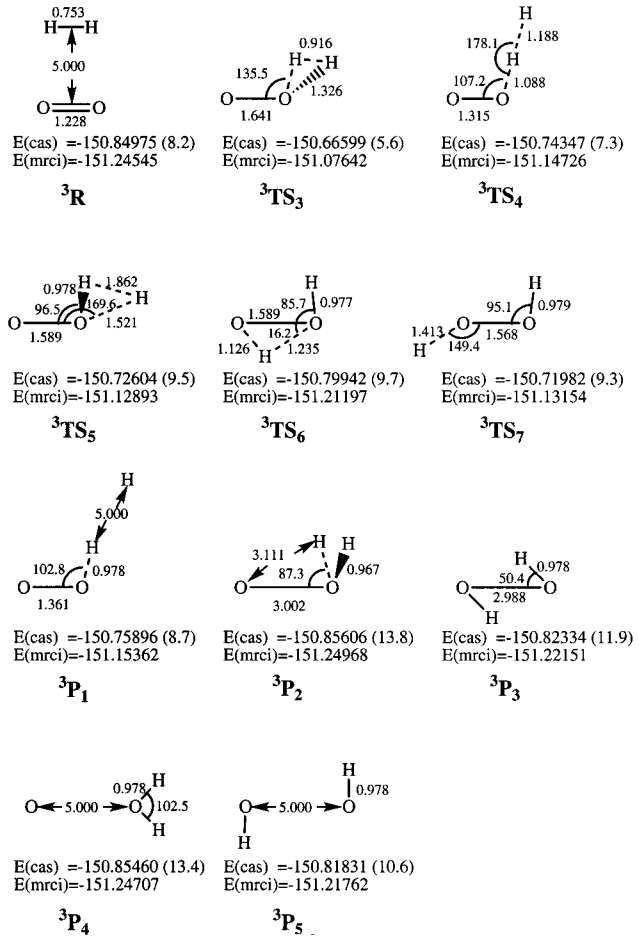

Figure 1. Molecular structures (angströms, degrees) and total CASSCF and MR-(S)DCI energies (Hartrees) of triplet critical species. In parentheses are the CASSCF zero-point vibrational energies in kcal/mol (1 Hartree = 627.5 kcal/mol).

filled in the product. This orbital crossing results in a very sharp increase of energy along the reaction coordinate and at Z_1Z_2 distances of ca. 1.5 Å the energy rises above the dissociation energy D_e of the H_2 molecule, 96.1 kcal/mol using CASSCF and 108.5 kcal/mol using MR-(S)DCI. This has been revealed by a two-dimensional potential surface scan along the HZ_1 and Z_1Z_2 distances (Scheme 1) with the two remaining geometry parameters optimized at the CASSCF level. In the interval of Z_1Z_2 distances between 1.1 and 1.4 Å, the potential surface is characterized by a huge hill as high as ca. 130−140 kcal/mol above the reactants (^{3}**R**) level which decreases gradually from short (0.35 Å) to long (1.35 Å) HZ_1 distances. Thus, the direct transition from the reactants to products on the triplet surface is unlikely to occur through a transition state (even if such a state may be found on the potential hill). If at all this will occur through a complete dissociation of the H_2 molecule. However, the latter opportunity does not seem chemically feasible, and it can be suggested that on the triplet surface the O_2 and H_2 molecules interact by alternative mechanisms discussed below.

On the singlet surface (Scheme 3) the concerted reaction leads to the formation of the hydrogen peroxide **^{1}P$_3$** in its ground ^{1}A state, with 34.7 kcal/mol (47.4 kcal/mol) of exothermicity. The active orbitals of the reactants **^{1}R** and product **^{1}P$_3$** are sketched in Scheme 5. Unlike the previous case, the reaction may proceed now through a symmetry-forbidden or through a symmetry-allowed transition state. This is because in the singlet oxygen molecule the two degenerate π^* orbitals share a singlet electron pair and as the hydrogen molecule approaches O_2 one of the

SCHEME 4: Orbitals and Symmetry Assignments for a Concerted Addition on the Triplet Surface

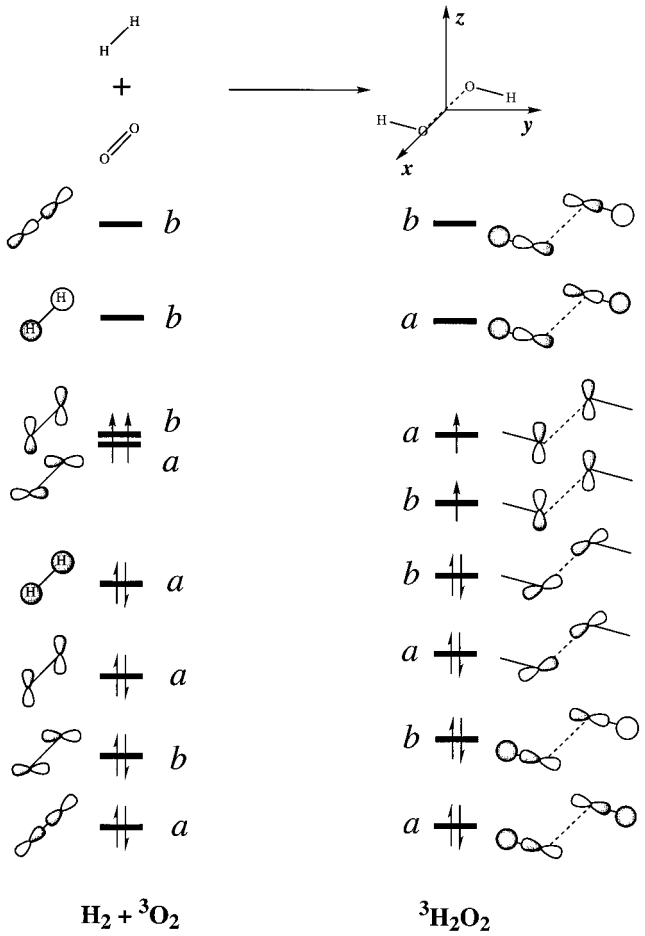

orbitals may become doubly occupied leaving another one empty. If the doubly occupied orbital is π_z^*, which belongs to the *b* irreducible representation, then the reaction is symmetry-allowed, and, alternatively, if the *a*-symmetric π_y^* orbital accommodates an electron pair, the reaction is symmetry-forbidden.[21]

For the given reaction, we managed to locate both transition states at the (14,10)CASSCF/6-31G** level as shown in Scheme 3 and Figure 2. One, for the symmetry-forbidden pathway, is the diradicaloid planar transition state **^{1}TS$_1$** (C_{2v} symmetric). The second is a twisted symmetry-allowed transition state **^{1}TS$_2$**. The diradicaloid transition state **^{1}TS$_1$** is characterized by a significantly elongated O−O bond (1.711 Å) with the H−H and O−H distances of 0.860 and 1.541 Å, respectively. In the symmetry-allowed transition state **^{1}TS$_2$** the O−O and H−H bonds are elongated more uniformly and acquire the values of 1.315 and 1.183 Å with the O−H distance of 1.505 Å (see Figure 2).

Both transition states lie slightly below the H_2 dissociation limit [the dissociation energy D_e in CASSCF is 96.1 kcal/mol and in MR-(S)DCI is 108.5 kcal/mol in fair agreement with the experimental value of 109 kcal/mol for D_e[22]] with the diradicaloid state at 90.3 kcal/mol (85.7 kcal/mol) and the symmetry-allowed one at 86.6 kcal/mol (73.5 kcal/mol) with respect to the singlet state reactants **^{1}R**. Both transition states were characterized by a vibrational analysis at the (14,10)CASSCF/6-31G** level which revealed that only the diradicaloid state **^{1}TS$_1$** is a first-order saddle point with the imaginary frequency of i2979 cm^{-1} and the transition vector that corresponds to a synchronous motion of the hydrogen atoms

SCHEME 5: Orbitals and Symmetry Assignments for a Concerted Addition on the Singlet Surface

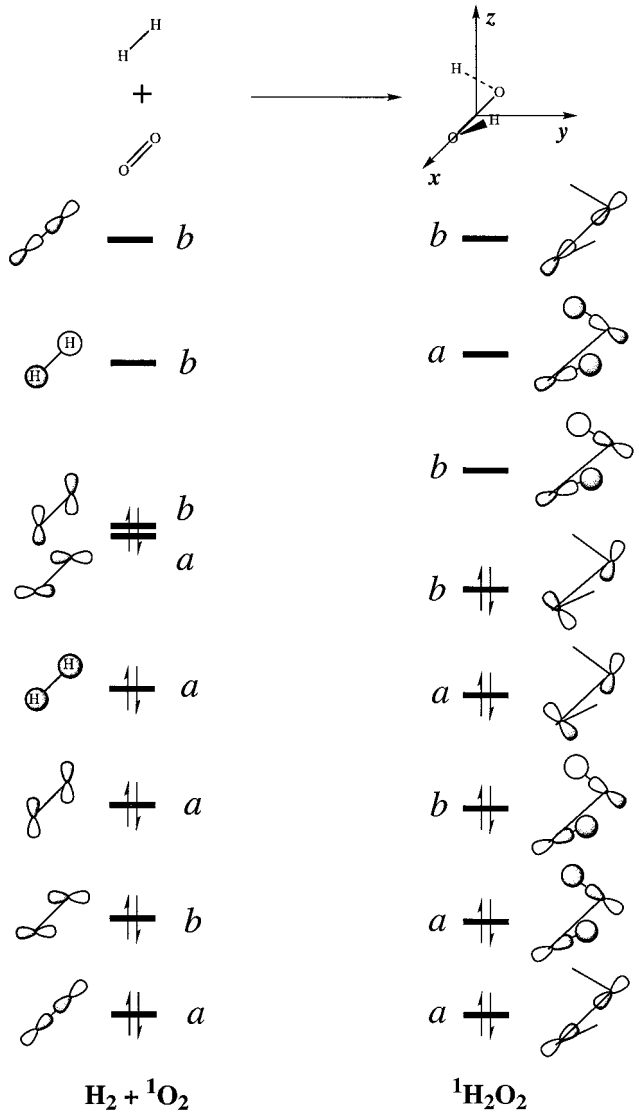

along the *z* axis (see Scheme 1). The symmetry-allowed transition state ^{1}**TS$_2$** is characterized by two imaginary frequencies. One of the vibrations (*i*5105 cm^{-1}) corresponds to a synchronous motion of the two hydrogens toward the oxygen atoms, and another one (*i*1542 cm^{-1}) corresponds to an asynchronous motion leading to the hydrogen abstracting transition state considered below for the "rebound" mechanism.

While the finding of ^{1}**TS$_1$** and ^{1}**TS$_2$** is theoretically interesting, we cannot assign to these transition states any chemical significance, because both lie too high in energy (more than 100 kcal/mol with respect to the triplet reactants ^{3}**R**). Together with the failure to locate any reasonable transition structure on the triplet surface, this finding implies that the concerted addition does not play any significant role in the interaction between O_2 and H_2. These extremely high barriers are very different as compared with the tiny barriers for the addition of H_2 to FeO^+.[10d−g,23]

2. Oxene Insertion Pathway. The oxene insertion pathway (shown with wavy lines in Schemes 2 and 3) leads from the reactants, ^{3}**R** and ^{1}**R**, to the oxywater molecule,[24] ^{3}**P$_2$** and ^{1}**P$_2$**. The oxygen molecule lies along the *z* axis of the coordinate system and the hydrogen molecule is parallel to the *y* axis such that the *xz* plane traverses the H−H bond (Scheme 1). The symmetry along this route is C_s.

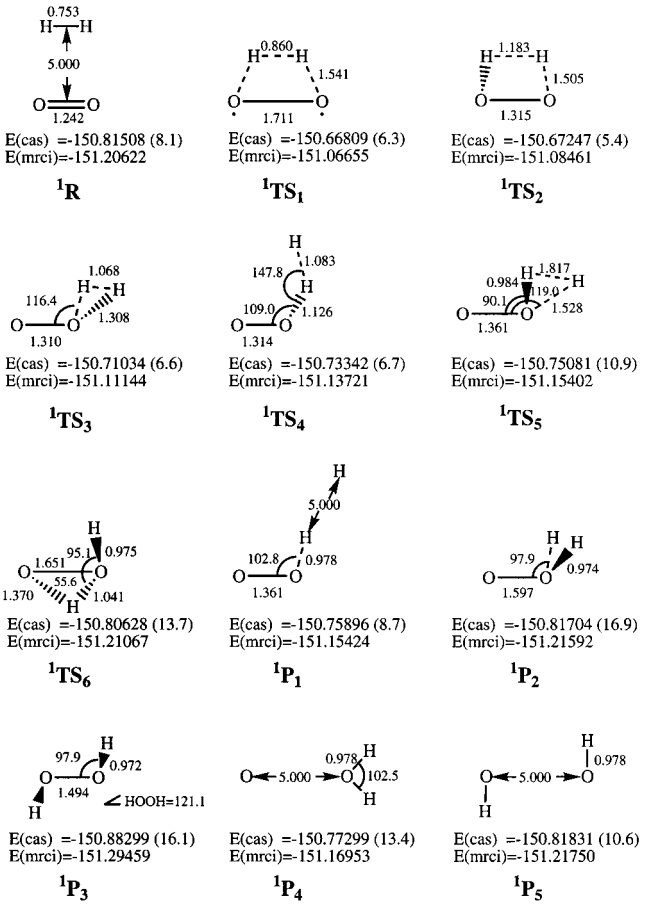

Figure 2. Molecular structures (angströms, degrees) and total CASSCF and MR-(S)DCI energies (Hartrees) of singlet critical species. In parentheses are the CASSCF zero-point vibrational energies in kcal/mol (1 Hartree = 627.5 kcal/mol).

As the hydrogen molecule approaches the triplet dioxygen (Scheme 2), the electron pair in the σ-bonding orbital of H_2 experiences strong repulsion with the electrons in π_x and π_x* orbitals of O_2. Electron delocalization from the oxygen π_y and π_y* orbitals into the σ* orbital of H_2 stabilizes slightly the transition structure, but at the CASSCF level this is still not enough to place the transition state below the dissociation energy of H_2 [the dissociation energy D_e in CASSCF is 96.1 kcal/mol and in MR-(S)DCI is 108.5 kcal/mol]. Despite a very high energy of 112.6 kcal/mol (103.4 kcal/mol), we managed to locate the second-order transition state ^{3}**TS$_3$** for this pathway. It is characterized by a relatively short H−H distance of 0.916 Å, a quite long O−O distance of 1.641 Å, and two imaginary frequencies of *i*2486 cm^{-1} and *i*744 cm^{-1}. The eigenvectors of the Hessian correspond to a translational motion of H_2 toward the oxygen and to a rotation of H_2 around the middle of the H−H bond, respectively. Thus, if the C_s constraint is lifted, this structure will collapse to one of the "rebound" transition states, most likely to ^{3}**TS$_5$** (see below).

The product of this step is the triplet oxywater molecule ^{3}**P$_2$** with an O−O distance of 3.002 Å at the (14,10)CASSCF/6-31G** level (Figure 1). This species may possibly be viewed as an $H_2O\cdots{}^3O$ cluster stabilized by a weak electrostatic interaction between the apical oxygen and the hydrogens of the water molecule (Figure 1). The relative energy of the triplet oxywater with respect to a triplet oxygen atom and a water molecule (^{3}**P$_4$**) is only 0.7 kcal/mol at the CASSCF level and 1.4 kcal/mol at the MR-(S)DCI level. It is thus conceivable that the obtained minimum is an artifact of the calculation (BSSE

effect) and that the energy surfaces from ^{3}**TS$_5$** and ^{3}**TS$_3$** lead directly to ^{3}**P$_4$** ($^3O + H_2O$).

On the singlet potential energy surface, the barrier for oxene insertion is considerably lower than in the triplet case. From the CASSCF calculation, the C_s symmetric transition state ^{1}**TS$_3$** lies only 64.1 kcal/mol [57.9 kcal/mol from MR-(S)DCI] above the singlet reactants ^{1}**R**. As the hydrogen molecule approaches O_2, the electrons delocalized initially in the π_x* and π_y* orbitals of the oxygen molecule sets in the π_y* orbital. Thus, the repulsion with the electron pair in the hydrogen σ orbital is reduced and an additional stabilization due to interaction with the empty σ* orbital is achieved. The H−H distance of 1.068 Å is markedly longer and the O−O distance of 1.310 Å is shorter than in the triplet transition state ^{3}**TS$_3$**. Despite the greater stability of ^{1}**TS$_3$** as compared to ^{3}**TS$_3$**, the ^{1}**TS$_3$** is still characterized by two imaginary frequencies of i1946 cm^{-1} and i1602 cm^{-1} that correspond to the same eigenvectors of the molecular Hessian as were discussed in the triplet case.

The singlet oxywater molecule ^{1}**P$_2$** is a relatively stable species that is 7.5 kcal/mol (2.7 kcal/mol) above the singlet reactants and 24.2 kcal/mol (25.6 kcal/mol) below the level of a singlet oxygen atom and a water molecule (^{1}**P$_4$**). The O−O bond length of 1.597 Å is nearly twice as short compared to the triplet case. These results are in fair agreement with the previously reported studies of the oxywater molecule.[24,25]

Concluding this subsection, it appears that the C_s symmetric oxene insertion mechanism will not play a significant role in the reaction between O_2 and H_2: First, because both transition states found are second-order saddle points, and as such do not connect two minima on the potential energy surface, rather a minimum corresponding to the reactants and a lower nonsymmetric transition state. Second, both second-order saddle points are still high in energy. A similar conclusion was drawn for the oxene insertion of FeO^+ and H_2.[10e] However, the energetics of the FeO^+ reaction is significantly more favorable as compared with the corresponding reaction of O_2 and H_2.

3. "Rebound" Mechanism. For this mechanism, we considered the in-plane approach of the hydrogen to oxygen molecule (Scheme 1). We did not impose any symmetry constraints on the "rebound" structures, which nevertheless came out as C_s symmetric.

The first step is the hydrogen abstraction (**TS$_4$** on both surfaces) that leads to triplet and singlet OOH + H radical pairs (**P$_1$**). The step is endothermic by +57.4 kcal/mol (+58.0 kcal/mol) and +35.7 kcal/mol (+33.1 kcal/mol) on the triplet and singlet surfaces, respectively. The barrier to the abstraction is lower on the singlet surface, 49.8 kcal/mol (41.9 kcal/mol) vs 65.8 kcal/mol (60.7 kcal/mol) on the triplet one. However, in absolute energy scale, the ^{1}**TS$_4$** is still 5.7 kcal/mol [CASSCF and MR-(S)DCI] higher in energy than the ^{3}**TS$_4$** such that intersystem crossing cannot occur along the reaction coordinate. Although the triplet and singlet radical pairs, ^{3}**P$_1$** and ^{1}**P$_1$**, are degenerate, we did not attempt calculation of the spin-interconversion rate in these pairs, because both radicals, OOH and H, are free and dynamics should be included to obtain meaningful results. Once again, the hydrogen abstraction reactivity of O_2 and H_2 differs from the corresponding reactivity of FeO^+ and H_2[10e] where the energetics are favorable and where high-spin and low-spin surfaces intersect along the hydrogen abstraction reaction coordinate.

The radical pairs face two possibilities. The first one is the rebound of the hydrogen atom to the oxygen atom that already binds one hydrogen (**TS$_5$**). This way leads to the singlet oxywater molecule (^{1}**P$_2$**). Then the oxywater can undergo an additional rearrangement (^{1}**TS$_6$**) leading to the singlet hydrogen peroxide (^{1}**P$_3$**). Alternatively, the oxywater can react with another hydrogen molecule yielding one more water molecule. A dissociation of the singlet oxywater molecule to an oxygen atom in the singlet state and a water molecule is unlikely due to a high energy demand of 24.2 kcal/mol (25.6 kcal/mol). In general, the results considered are in a reasonable agreement with the studies of the oxywater rearrangements reported previously by Schwarz et al.[24] and by Schaefer et al.[25]

Another type of H-rebound step leads directly from the radical pair to the hydrogen peroxide (**P$_3$**). On the triplet surface, this step proceeds via a high potential barrier (^{3}**TS$_7$**). This is understandable since in the triplet hydrogen peroxide the two OH fragments are virtually unbound. The binding energy is only 1.9 kcal/mol (1.2 kcal/mol) with respect to two OH radicals (^{3}**P$_5$**). The O−O distance in the triplet H_2O_2 is 2.988 Å. Thus, during this step there occurs formation of one O−H bond (another one already exists) with simultaneous dissociation of the O−O bond in the OOH radical. This explains the existence of a high activation barrier on the triplet surface. On the singlet surface, this step is barrierless. We calculated a number of points along this pathway, at the CASSCF level, fixing the distance between the free hydrogen atom and the terminal oxygen atom (from 5 Å to optimal value of 0.978 Å) and optimizing all other geometry variables. This scan revealed that the energy of the singlet "rebound" decreases monotonically. This difference between the "rebound" mechanisms on the high-spin and low-spin surfaces has been noted also for the CH_4 oxidation by the active species of the P450 enzyme.[26]

Thus, the "rebound" mechanism seems to be the most favorable mode of reaction between O_2 and H_2. It leads to a variety of products that can participate in subsequent chain reactions. However, the limiting step in this mechanism, the H-abstraction step, is endothermic by more than 30 kcal/mol and its activation energy is too high [65.8 kcal/mol (60.7 kcal/mol) on the triplet surface and 49.8 kcal/mol (41.9 kcal/mol) on the singlet surface] to induce any noticeable reactivity of the O_2 and H_2 mixture at the standard conditions. The rate constant for the fastest process (triplet rebound) would be 10^{-19} mol^{-1} s^{-1} at room temperature. A somewhat faster rate is expected if tunneling becomes important.[27] Using the Wigner's or Bell's formulas,[28] the tunneling correction would enhance the rate by an order of magnitude[29] to $\sim 10^{-18}$ mol^{-1} s^{-1}, which is still too slow to disturb the kinetic persistence of the O_2/H_2 mixture.

4. Conclusions

We have asked at the outset what is the reason for the kinetic stability of a O_2/H_2 mixture and used high level calculations to seek an answer. Three possible mechanisms of reactions between hydrogen and oxygen molecules were considered: (i) the concerted addition, (ii) the oxene insertion, and (iii) the "rebound" mechanisms. The calculations revealed that the first two mechanisms, which lead to the most stable oxidation products, do not play any significant role in the oxidation reaction since their transition structures are highly energetic and are characterized by two imaginary frequencies. As such, they do not correspond to true transition structures and have a channel down to the corresponding hydrogen abstraction transition states of the "rebound" mechanism.

The only reaction potentially available to the O_2/H_2 mixture is via the "rebound" mechanism. The "rebound" mechanism consists of two stages, hydrogen abstraction and hydrogen rebound. The hydrogen abstraction step that leads to the

OOH + H radical pair is highly endothermic (>30 kcal/mol) and can hardly be expected to yield a marked concentration of radical pairs at normal temperatures and pressures. Furthermore, no intersystem crossing occurs en route to the H-abstraction product. Thus, the low-lying singlet state does not assist to abstract a hydrogen atom.

The rebound step on the triplet surface is characterized by higher activation barriers than on the singlet surface irrespective of the site of rebound (to oxywater or to hydrogen peroxide). Thus, the spin-interconversion in the OOH + H radical pair to the singlet state may facilitate the H-rebound step. However, the short-range spin−orbit coupling can hardly be expected to be responsible for such a spin-flip. The assessment of the spin-interconversion rate in such a case should include dynamic effects and goes beyond the scope of the present study.

Thus, in answer of the questions posed at the opening, our results clearly show that the direct insertion of the oxygen into H−H bond is unlikely. If at all feasible, an exceedingly slow oxidation process can occur via the "rebound" mechanism in a stepwise manner and involves free radicals. The lowest singlet state of the oxygen does not facilitate the initial steps of the three reaction mechanisms considered. These reactivity patterns are entirely different from the reactions of oxidants such as FeO^+ [7,30] and mono-oxygenase enzymes.[2−6,26] The latter two oxidants have low-lying vacant orbitals that lower the corresponding reaction barriers.[10e,30,31] Thus, the coordinatively unsaturated FeO^+ has empty d orbitals[10e] and compound I of the enzyme cytochrome P450 has a half-filled porphyrin orbital that serves the same function.[30,31] In contrast, O_2 is electronically saturated and evidently its π^* orbitals are still too high to function in the same manner as the empty d orbitals of FeO^+ or the porphyrin "hole" of compound I. It follows, therefore, that the origins of the reactivity difference between the oxidants may be traced to this specific fundamental difference in the electronic structures of O_2 as compared with FeO^+ or with compound I of the enzyme cytochrome P450.

Acknowledgment. The research is supported by a common grant (to S.D.P. and S.S.) from GIF, the German Israeli Foundation. Partial support is provided in Jerusalem also by the VW Stiftung (to S.S.).

References and Notes

(1) Atkins, P. W. *Physical Chemistry*, 5th ed.; Oxford University Press: Oxford, 1994.

(2) Woggon, W. D. *Top. Curr. Chem.* **1996**, *184*, 40.

(3) *Cytochrome P-450: Structure, Mechanisms and Biochemistry*; Ortiz de Montellano, P. R., Ed.; Plenum: New York, 1986.

(4) Sono, M.; Roach, M. P.; Coulter, E. D.; Dawson, J. H. *Chem. Rev.* **1996**, *96*, 2841.

(5) (a) Groves, J. T.; Zhang Han, Y.-Z., Chapter 1 in ref 3. (b) Groves, J. T. *J. Chem. Educ.* **1985**, *62*, 928.

(6) Meunier, B. *Chem. Rev.* **1992**, *92*, 1411.

(7) Schröder, D.; Schwarz, H. *Angew. Chem., Int. Ed. Engl.* **1995**, *34*, 1973.

(8) *Gmelins Handbuch der Anorganischen Chemie. 8. Auflage. Sauerstoff*; Pietch, E., Ed.; Verlag Chemie: Weinheim, 1943.

(9) (a) Bell, R. P. *Proc. R. Soc. A* **1935**, *148*, 241. (b) Evans, M. G.; Polanyi, M. *Trans. Faraday Soc.* **1935**, *31*, 875.

(10) For the role of SOC in analogous bond activation reactions, see (a) Danovich, D.; Shaik, S. *J. Am. Chem. Soc.* **1997**, *119*, 1773. (b) Armentrout, P. B.; *Science* **1991**, *251*, 175. (c) Wiesshaar, J. C. *Acc. Chem. Res.* **1993**, *26*, 213. (d) Fiedler, A.; Schroder, D.; Schwarz, H.; Shaik, S. *J. Am. Chem. Soc.* **1994**, *116*, 10734. (e) Filatov, M.; Shaik, S. *J. Phys. Chem. A* **1998**, *102*, 3835. (f) Yoshizawa, K.; Shiota, Y.; Yamabe, T. *J. Am. Chem. Soc.* **1998**, *120*, 564−572; Yoshizawa, K.; Shiota, Y.; Yamabe, T. *Organometallics* **1998**, *17*, 2825−2831; Yoshizawa, K.; Shiota, Y.; Yamabe, T. *Chem. Eur. J.* **1997**, *3*, 1160. (g) Shaik, S.; Danovich, D.; Fiedler, A.; Schroder, D.; Schwarz, H. *Helv. Chim. Acta* **1995**, *78*, 1393.

(11) Shaik, S.; Filatov, M.; Schröder, D.; Schwarz, H. *Chem. Eur. J.* **1998**, *4*, 193−199.

(12) Collman, J. P.; Chien, A. S.; Eberspacher, T. A.; Brauman, J. I. *J. Am. Chem. Soc.* **1998**, *120*, 425.

(13) (a) MOLPRO is a package of ab initio prorgams written by Werner, H.-J., and Knowles, P. J., with contributions from Amos, R. D.; Bernhardsson, A.; Berning, A.; Celani, P.; Cooper, D. L.; Deegan, M. J. O.; Dobbyn, A. J.; Eckert, F.; Hampel, C.; Hetzer, G.; Korona, T.; Lindh, R.; Lloyd, A. W.; McNicholas, S. J.; Manby, F. R.; Meyer, W.; Mura, M. E.; Nicklass, A.; Palmieri, P.; Pitzer, R.; Rauhut, G.; Schütz, M.; Stoll, H.; Stone, A. J.; Tarroni, R.; Thorsteinsson, T. (b) Werner, H.-J.; Knowles, P. J. *J. Chem. Phys.* **1985**, *82*, 5053. (c) Knowles, P. J.; Werner, H.-J. *Chem. Phys. Lett.* **1985**, *115*, 259.

(14) Schmidt, M. W.; Baldridge, K. K.; Boatz, J. A.; Elbert, S. T.; Gordon, M. S.; Jensen, J. H.; Koseki, S.; Matsunaga, N.; Nguyen, K. A.; Su, S. J.; Windus, T. L.; Dupuis, M.; Montgomery, J. A. *GAMESS−USA Rev.* Feb. 1995.

(15) Hehre, W. J.; Radom, L.; Schleyer, P. von R.; Pople, J. A. *Ab Initio Molecular Orbital Theory*; Wiley-Interscience: New York, 1986.

(16) Hanrath, M.; Engels, B. *Chem. Phys.* **1997**, *225*, 197.

(17) Dunning, T. H., Jr. *J. Chem. Phys.* **1989**, *90*, 1007.

(18) Davidson, E. R. *Adv. Quantum Chem.* **1972**, *6*, 235.

(19) Herzberg, G. *Electronic Spectra and Electronic Structure of Polyatomic Molecules*; van Nostrand: Princeton, New Jersey, 1966.

(20) Atkinson, R.; Baulch, D. L.; Cox, R. A.; Hampson, R. F., Jr.; Kerr, J. A.; Troe, J. *J. Phys. Chem. Ref. Data* **1992**, *21*, 1125.

(21) Harding, L. B.; Goddard, W. A., III. *J. Am. Chem. Soc.* **1980**, *102*, 439.

(22) Huber, K.-P.; Herzberg, G. *Constants of Diatomic Molecules*; van Nostrand-Reinhold: New York, 1979.

(23) (a) Clemmer, D. E.; Chen, Y.-M.; Khan, F. A.; Armentrout, P. B. *J. Phys. Chem.* **1994**, *98*, 6522. (b) Schröder, D.; Schwarz, H.; Clemmer, D. E.; Chen, Y.; Armentrout, P. B.; Baranov, V. I.; Bohme, D. K. *Int. J. Mass Spectrom. Ion Proc.* **1997**, *161*, 175.

(24) Schröder, D.; Schalley, C. A.; Goldberg, N.; Hrûsák, J.; Schwarz, H. *Chem. Eur. J.* **1996**, *2*, 1235.

(25) Huang, H. H.; Xie, Y.; Schaefer, H. F. III. *J. Phys. Chem.* **1996**, *100*, 6076.

(26) Harris, N.; Cohen, S.; Ogliaro, F.; Filatov, M.; Shaik, S. *Angew. Chem., Int. Ed. Engl.* **2000**, *39*, 2003.

(27) See, for example, tunneling effects in reactions of hydrogen abstraction by oxygen in Garrett, B. C.; Truhlar, D. G.; Bowman, J. M.; Wagner, A. F.; Robie, D.; Arepalli, S.; Presser, N.; Gordon, R. J. *J. Am. Chem. Soc.* **1986**, *108*, 3515.

(28) Melander, L.; Saunders, W. H. *Reaction Rates of Isotopic Molecules*; Wiley-Interscience: New York, 1980; pp 15−16.

(29) Using the highest imaginary frequency of the present study (*i*2979 cm^{-1} for ^{1}**TS$_1$**) Bell's correction amounts to 9.14 while Wigner's correction to 9.51.

(30) Schröder, D.; Shaik, S.; Schwarz, H. *Acc. Chem. Res.* **2000**, *33*, 139.

(31) Filatov, M.; Harris, N.; Shaik, S. *J. Chem. Soc., Perkin Trans. 2* **1999**, 399.